Supplementary Information

Role of hydrodynamics, Li+ addition and transformation kinetics on the formation of plate-like {001} calcite crystals

Nives Matijaković Mlinarić, Jasminka Kontrec, Branka Njegić Džakula, Giuseppe Falini, Damir Kralj

Table SI1. A brief derivation of equations 4-6.

$dl/dt = D\,V_m\,(c-c_S)\,/\,l$	$dl/dt = k_{ln}\,((c-c_S)-1)\,ln(c-c_S)$	$dl/dt = k_e\,(c/c_S)^{7/6}\,((c/c_S)\text{-}1))^{2/3}(\ln(c/c_S))^{1/6}$ $exp(\text{-}K_e/\ln(c/c_S))$

Difusion controled crystal growth is derived from Fick's first law. A flux of matter dn/dt, diffusing through the area A perpendicular to the x-axis is:	**Screw dislocation growth mechanism** assumed growth with no need for surface nucleation and the incorporation of growth units into the dislocation on crystal surfaces. The structure of crystal surface with spiral dislocation is characterized by the surface height, d, the average distance between the active growth sites, x_o, and the distance between two adjacent surfaces, y_o	**Polynuclear growth mechanism** assumed that the crystal surface is simultaneously covered by several circular nuclei of thickness d and constituent ions in equilibrium with solution. The linear growth rate is inversely proportional to time, τ, which takes to cover a surface A with a new layer:
$dn/dt = DA(dc/dx)$		$v_g = d/\tau = d((\pi J' v_\infty^2)/3)^{1/3}$
where D is the diffusion coefficient and dc/dx is the concentration gradient. In case of a sphere it is defined as:	$x_0 = d\,S^{1/2}\,exp(\gamma/k_BT)$	In the expression, J' is the rate of surface nucleation and v_∞ net lateral velocity of surface island growth
$dc/dx = (c-c_s)/r$	$y_0 = 19\,d\,\gamma/k_B\,T\,lnS,$	
Where r is the radius of the sphere. Deposition of the meter dn the volume of the sphere dV increases for dr.	where $S = c/c_s$. The surface concentration of active sites can be defined as:	$J' = (D_s/d^4)\,exp\,(-\Delta G'^*/kT),$
$dV = 4\,r^2\,\pi\,dr = V_m\,dn$	$1/x_0y_0 = S^{1/2}lnS/19d^2(\gamma/k_BT)exp(\gamma/k_BT).$	where D_s is the diffusion coefficient. By inserting J' and v_∞ one obtains:
For the sufrace of the sphere $A = 4r^2\pi$ it follows that the growth rate controlled by diffusion is proportional to the absolute supersaturation and inversely proportional to the particle size:	At higher relative supersaturations, $S^{1/2}\,lnS$ can be approximated with $(S-1)$:	$v_g = k_eS^{7/6}(S-1)^{2/3}(lnS)^{1/6}exp(-K_e/lnS)$
$dr/dt = D\,Vm\,(c-c_s)/r$	$1/x_0y_0 \approx (S-1)/19d^2(\gamma/k_BT)exp(\gamma/k_BT)$	where
	The rate of linear growth of the crystal surface is proportional to the rate of lateral growth of the surface (adsorption along the column) at supersaturation $S<1.6$ and $x_o<y_0$ the rate of lateral growth is proportional to $S-1 = c/c_s$ (and the density of the column y_0^{-1}:	$k_e = 2dv_{in}(K_{ad}c_sV_m)^{4/3}exp(-\gamma/kT)$
		v_{in} is the integration frequency, γ is the edge energy and
	$v_g \sim k_{ln}(S-1)lnS.$	$K_e = \pi\gamma^2/3k^2T^2.$

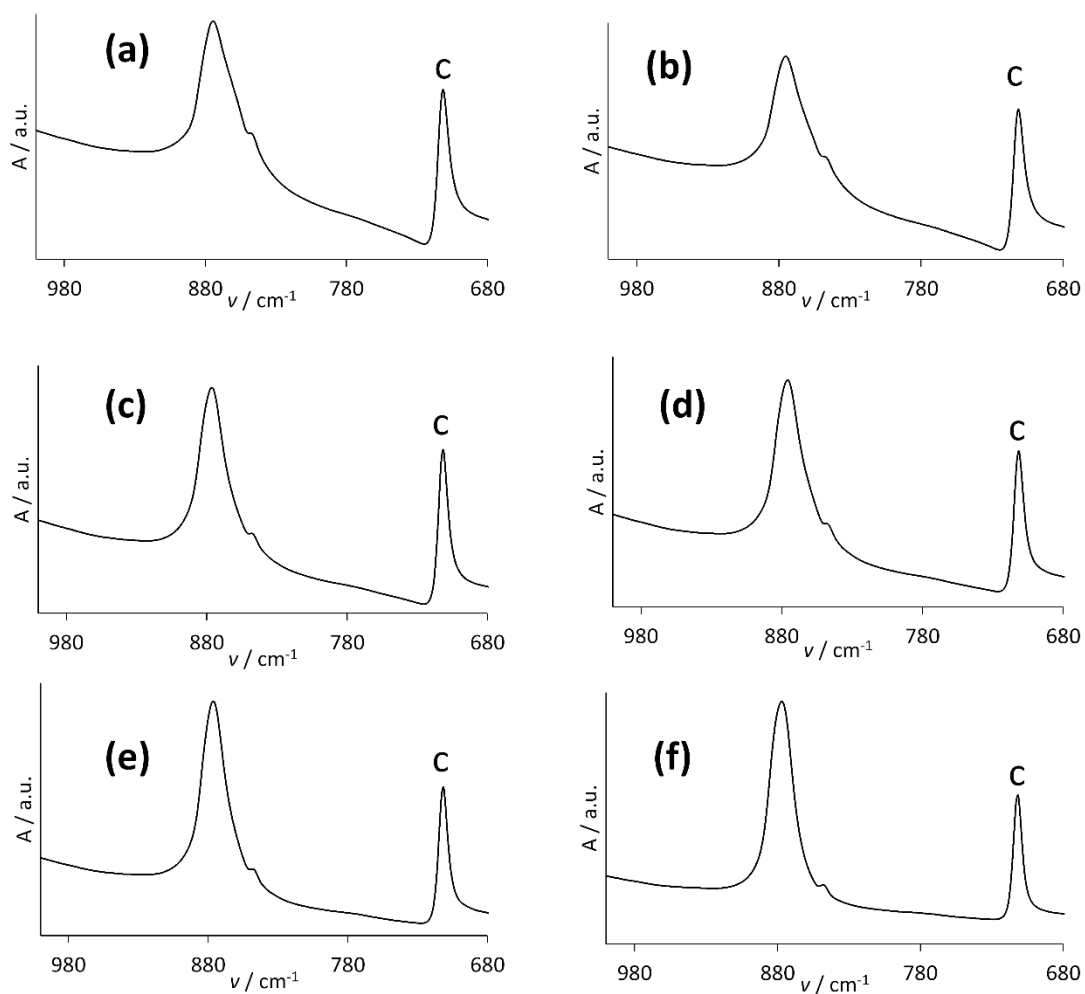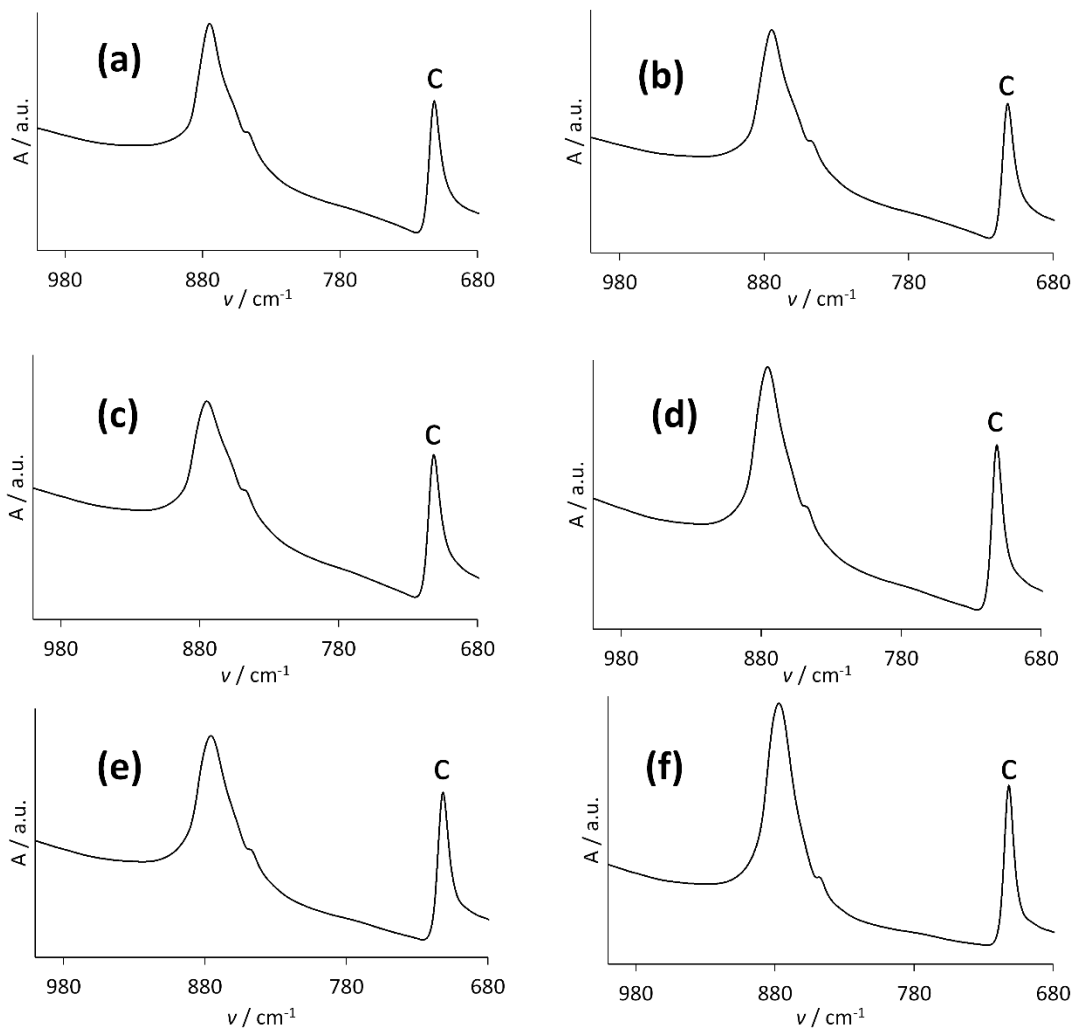**Figure SI1.** FTIR spectra of the precipitates obtained in the magnetically stirred (MAG) precipitation systems ($c_i(CaCl_2) = c_i(NaHCO_3) = 0.1$ mol dm^{-3}) after 5 days of aging. Different initial Li$^+$ concentrations have been applied: a) $c(Li^+) = 0.0$ mol dm^{-3}, b) $c(Li^+) = 0.1$ mol dm^{-3}, c) $c(Li^+) = 0.3$ mol dm^{-3}, d) $c(Li^+) = 0.5$ mol dm^{-3}, e) $c(Li^+) = 0.7$ mol dm^{-3} and f) $c(Li^+) = 1.0$ mol dm^{-3}. [#] c indicates calcite.

Figure SI2. FTIR spectra of the precipitates obtained in the mechanically stirred (MAG) precipitation systems ($c_i(CaCl_2) = c_i(NaHCO_3) = 0.1$ mol dm^{-3}) after 5 days of aging. Different initial Li$^+$ concentrations have been applied: a) $c(Li^+) = 0.0$ mol dm^{-3}, b) $c(Li^+) = 0.1$ mol dm^{-3}, c) $c(Li^+) = 0.3$ mol dm^{-3}, d) $c(Li^+) = 0.5$ mol dm^{-3}, e) $c(Li^+) = 0.7$ mol dm^{-3} and f) $c(Li^+) = 1.0$ mol dm^{-3}. [#] c indicates calcite.
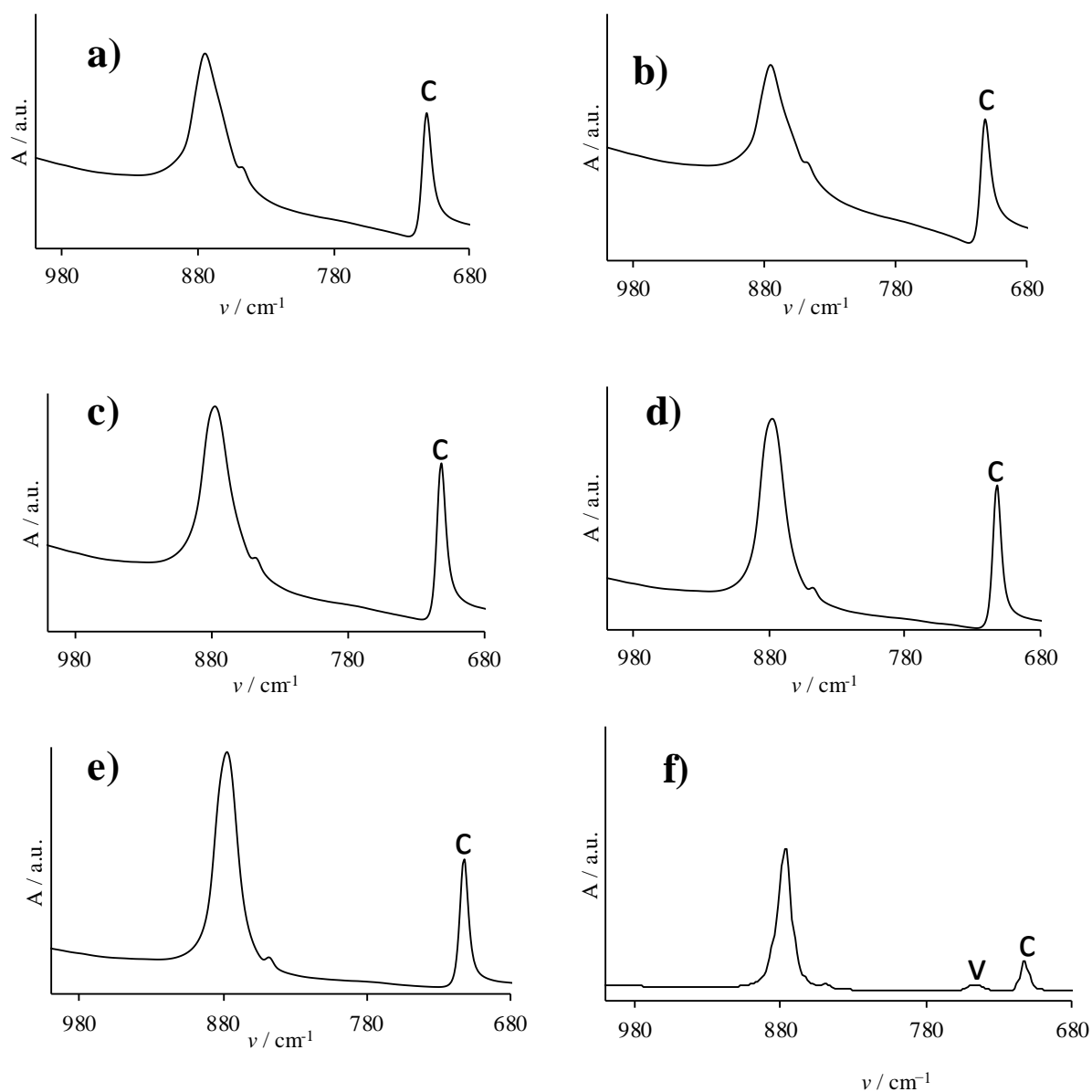
Figure SI3. FTIR spectra of the precipitates obtained in the ultrasonicated (US) precipitation systems (c_i(CaCl$_2$) = c_i(NaHCO$_3$) = 0.1 mol dm^{-3}) after 5 days of aging. Different initial Li$^+$ concentrations have been applied: a) c(Li$^+$) = 0.0 mol dm^{-3}, b) c(Li$^+$) = 0.1 mol dm^{-3}, c) c(Li$^+$) = 0.3 mol dm^{-3}, d) c(Li$^+$) = 0.5 mol dm^{-3}, e) c(Li$^+$) = 0.7 mol dm^{-3} and f) c(Li$^+$) = 1.0 mol dm^{-3}. [#] c indicates calcite. [*] v indicates vaterite.

Table SI2. Assignment of IR bands in FTIR spectra of precipitates obtained after 5 days of aging

.

Wavenumber/ cm^{-1}	Band assignment*
Calcite	
1425	ν_3, asymmetric C−O stretching mode
876	ν_2, CO$_3$ out of plane deformation mode
713	ν_4, O−C−O bending (in plane deformation) mode
Calcite and vaterite mixture	
1485	ν_3, asymmetric C−O stretching mode
1423	ν_3, asymmetric C−O stretching mode
1088	ν_1, symmetric C−O stretching mode
876	ν_2, CO$_3$ out of plane deformation mode
746	ν_4, O−C−O bending (in plane deformation) mode vaterite
713	ν_4, O−C−O bending (in plane deformation) mode calcite

*Band assignment were done according to F.A. Andersen, Lj. Brečević: Infrared spectra of amorphous and crystalline calcium carbonate, *Acta Chim. Scand.* **45** (1991) 1018-1024.

Table SI3. Polymorphic composition of $CaCO_3$ samples obtained by different stirring modes in precipitation systems, $c_i(CaCl_2)$ = $c_i(NaHCO_3)$ = 0.1 mol dm^{-3} and different LiCl content. Magnetically and mechanically stirred systems were agitated for 1 hour and ultrasonicated system for 10 minutes.

c(Li) / mol dm^{-3}	Stirring mode	w(calcite) / wt. %
0.0	MAG	52.57 ± 3.25
	US	89.91 ± 10.96
	MECH	98.17 ± 2.56
0.1	MAG	3.73 ± 5.38
	US	62.51 ± 3.75
	MECH	98.96 ± 2.97
0.3	MAG	4.92 ± 4.37
	US	11.37 ± 2.37
	MECH	55.19 ± 3.10
0.5	MAG	2.35 ± 4.69
	US	4.8 ± 0.10
	MECH	54.21 ± 4.02
0.7	MAG	2.32 ± 3.26
	US	2.62 ± 0.19
	MECH	53.40 ± 0.25
1.0	MAG	1.64 ± 2.57
	US	2.45 ± 0.23
	MECH	20.11 ± 0.63

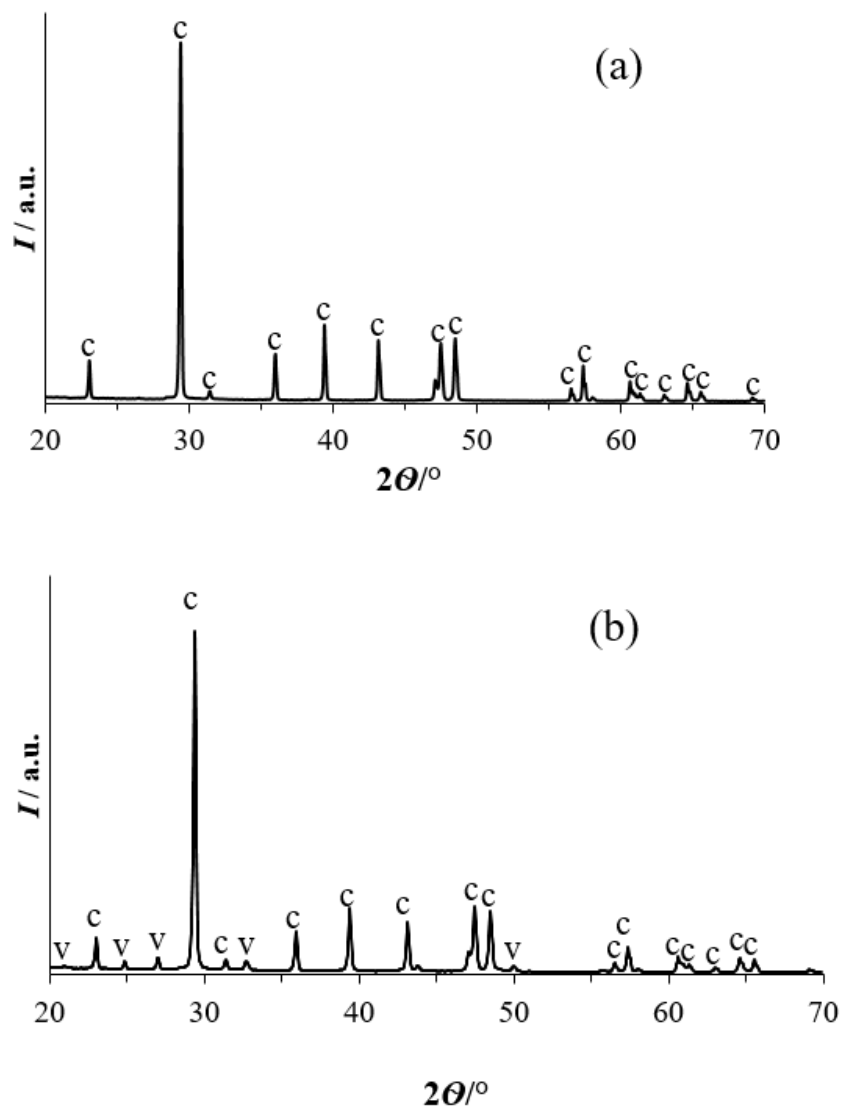**Figure SI4** PXRD diffractograms of the $CaCO_3$ precipitates obtained in the ultrasonicated (US) precipitation systems ($c_i(CaCl_2) = c_i(NaHCO_3) = 0.1$ mol dm^{-3}) after 5 days of aging: (a) representative pattern of the calcite samples obtained in the systems with initial Li$^+$ concentration, 0.0 mol dm$^{-3} < c_i < 0.7$ mol dm^{-3} and (b) pattern of the samples obtained in the systems with initial Li$^+$ concentration, $c_i = 1.0$ mol dm^{-3}. **v** indicates vaterite and **c** indicates calcite.
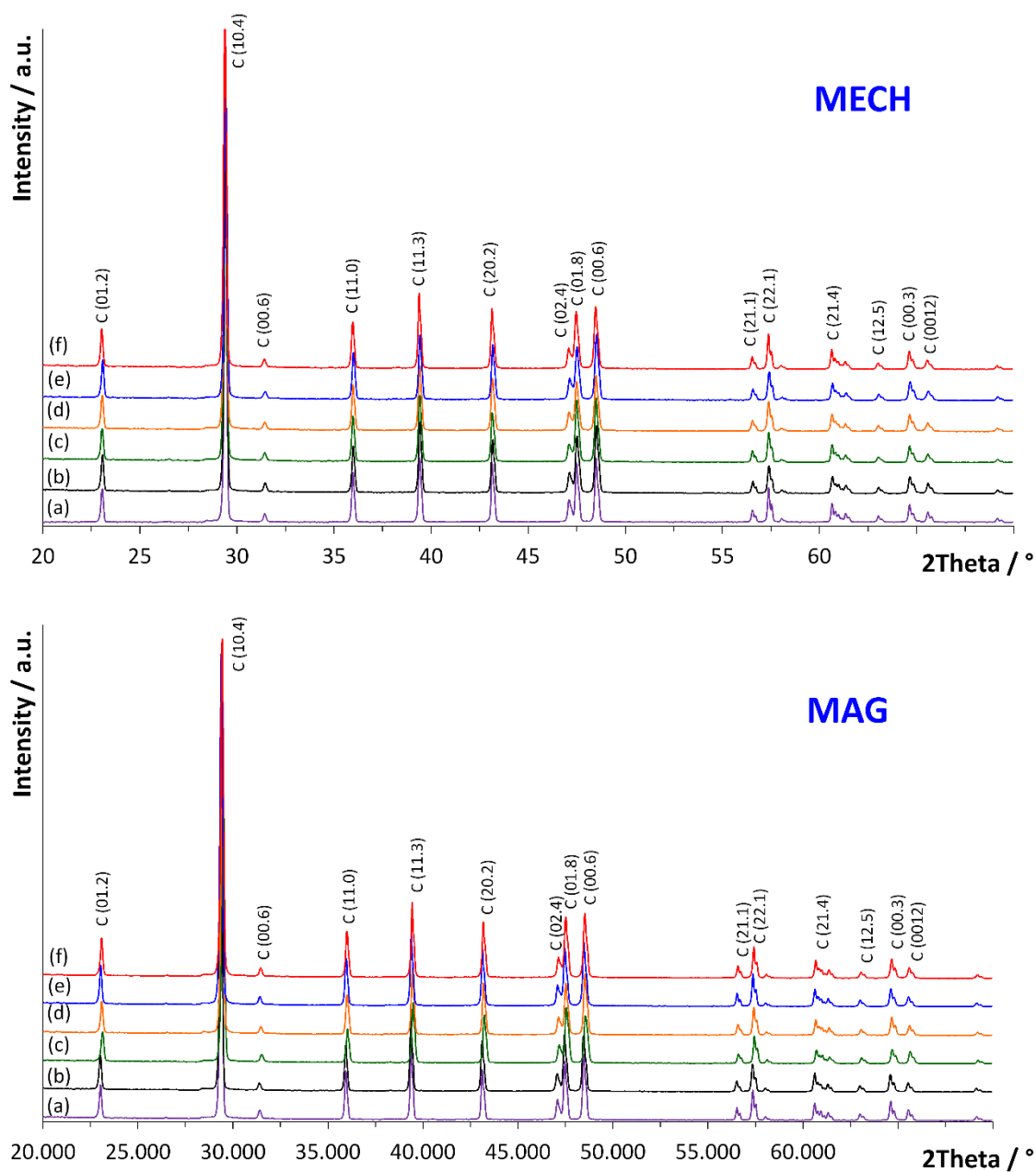
Figure SI5. PXRD diffractograms of the $CaCO_3$ precipitates obtained in the mechanically stirred (top) and magnetically stirred (bottom) precipitation systems ($c_i(CaCl_2) = c_i(NaHCO_3) = 0.1$ mol dm^{-3}) after 5 days of aging. Initial Li$^+$ concentration were (a) 0.0 mol dm^{-3}, (b) 0.1 mol dm^{-3}, (c) 0.3 mol dm^{-3}, (d) 0.5 mol dm^{-3}, (e) 0.7 mol dm^{-3} and (f) 1.0 mol dm^{-3}. The diffraction patterns were indexed accordingly to the PDF 00-005-0586. In all systems only calcite has been detected.

Table SI4. Assignment of peaks in PXRD patterns of all samples obtained after 5 days of aging and shown in Figures SI4 and SI5.

2θ / º	(hkl)
Calcite	
29.4	104
35.9	110
9.4	113
43.1	202
47.5	018
48.5	116
Calcite and vaterite mixture	
24.9	020
27.1	021
29.4	104
32.7	022
35.9	110
39.4	113
40.7	023
43.8	130
50.0	114
55.8	222

PXRD patterns were indexed according to JCPDS card No. 05-0586 (calcite) and JCPDS card No: 33-0268 (vaterite)
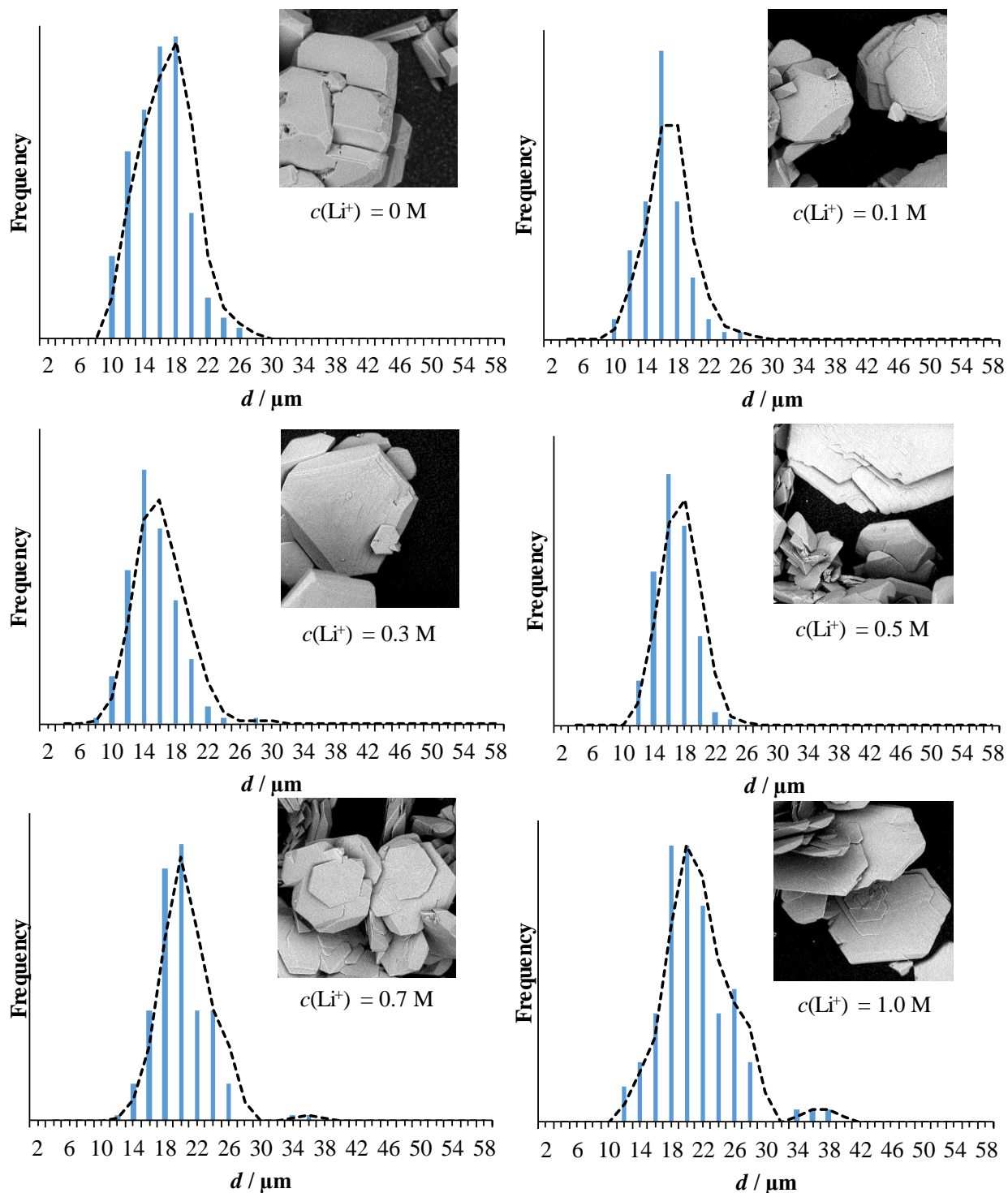
Figure SI6. Particle size distribution of calcium carbonate samples obtained in the magnetically stirred (MAG) precipitation systems ($c_i(CaCl_2) = c_i(NaHCO_3) = 0.1$ mol dm^{-3}) after 5 days of aging. Different initial Li$^+$ concentrations have been applied. Inserts show typical morphologies of the samples.
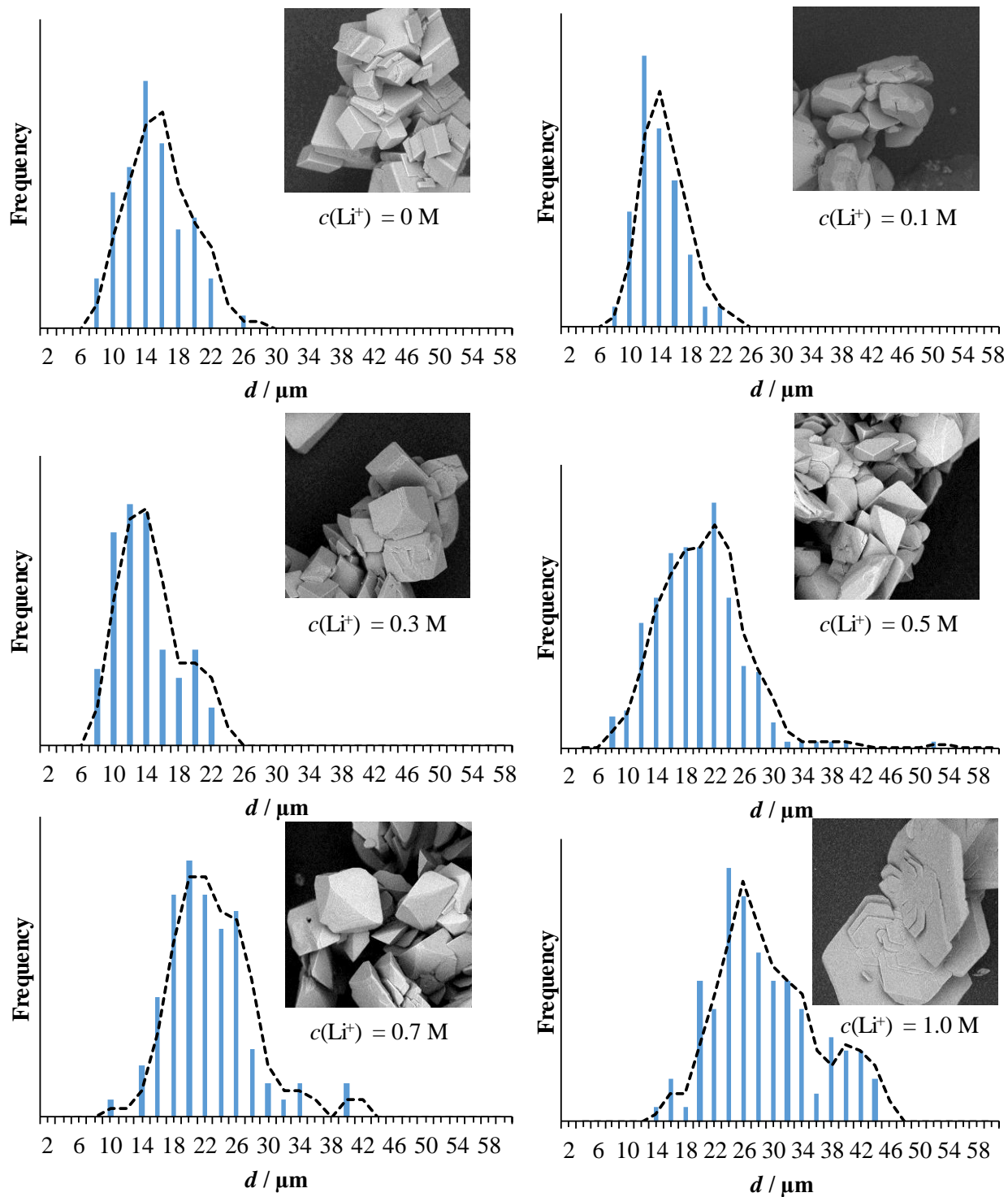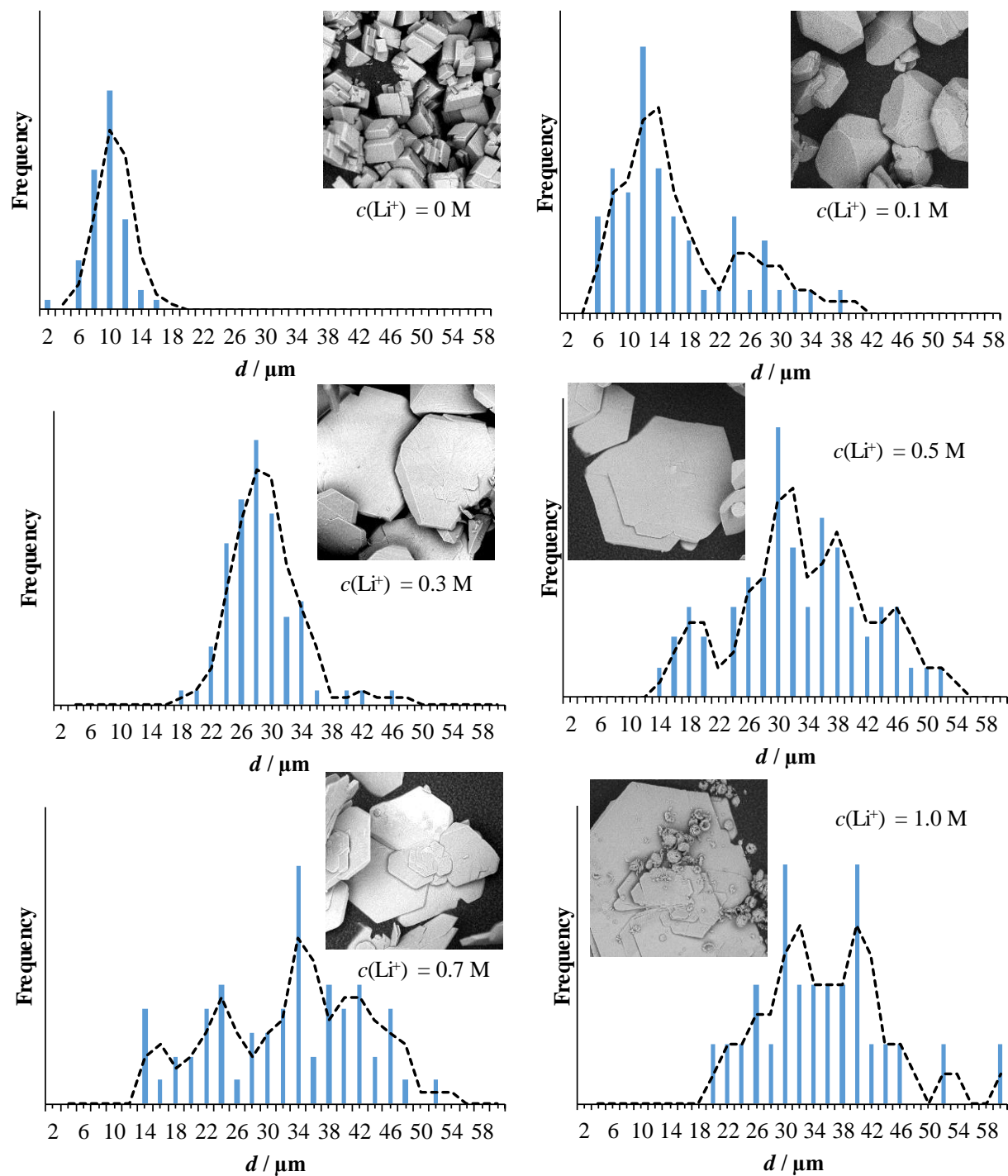
Figure SI7. Particle size distribution of calcium carbonate samples obtained in the mechanically stirred (MECH) precipitation systems ($c_i(CaCl_2) = c_i(NaHCO_3) = 0.1$ mol dm^{-3}) after 5 days of aging. Different initial Li$^+$ concentrations have been applied. Inserts show typical morphologies of the samples.
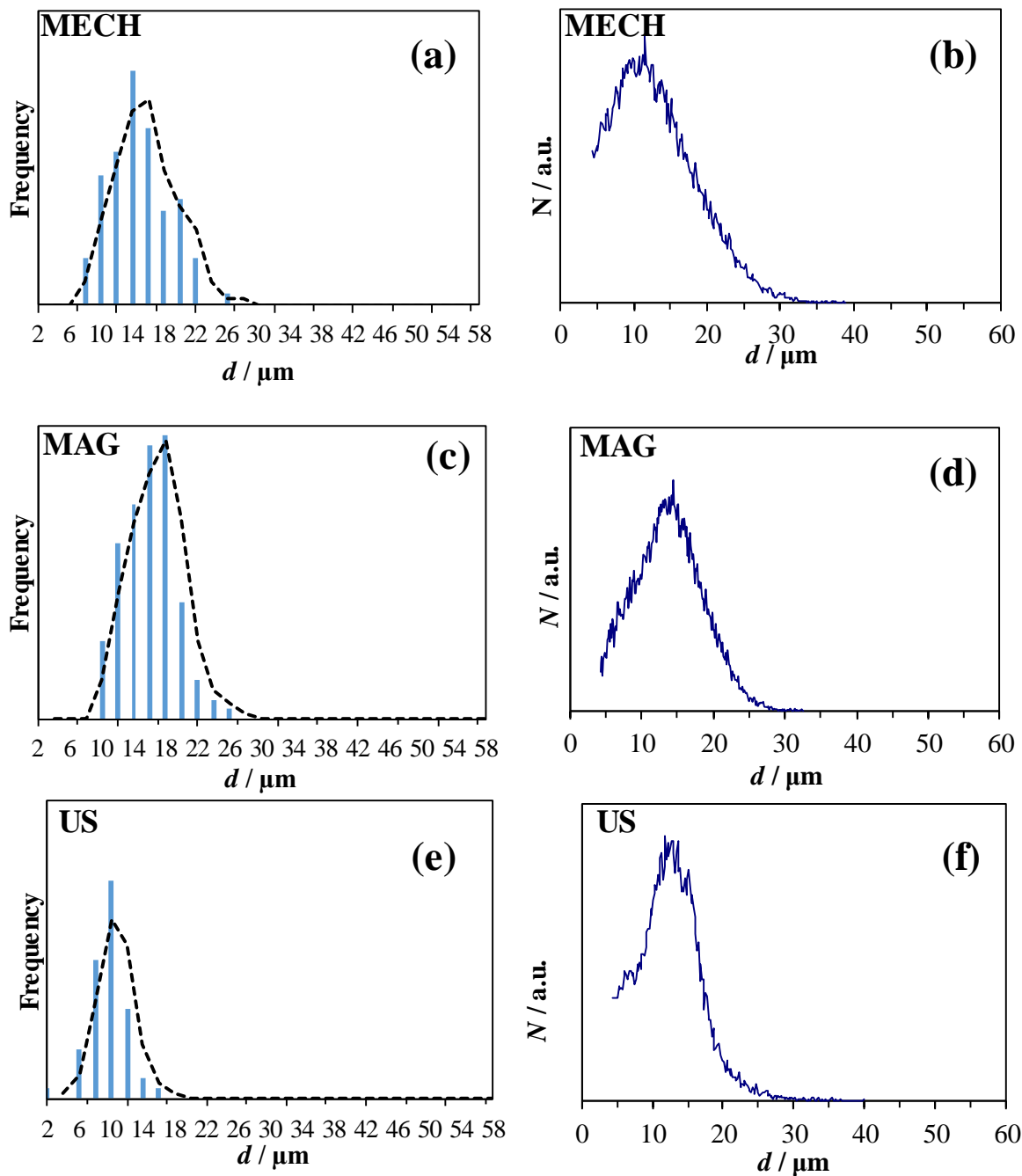
Figure SI8. Particle size distribution of calcium carbonate samples obtained in the ultrasonicated (US) precipitation systems ($c_i(CaCl_2) = c_i(NaHCO_3) = 0.1$ mol dm^{-3}) after 5 days of aging. Different initial Li$^+$ concentrations have been applied. Inserts show typical morphologies of the samples

Figure SI9. Comparison of particle size distribution of calcium carbonate samples in the precipitation systems, $c_i(CaCl_2) = c_i(NaHCO_3) = 0.1$ mol dm^{-3}, no LiCl addition, after 5 days of aging and different agitation modes: distributions obtained by ImageJ software; a); c); e) and Coulter Counter: b); d); f).
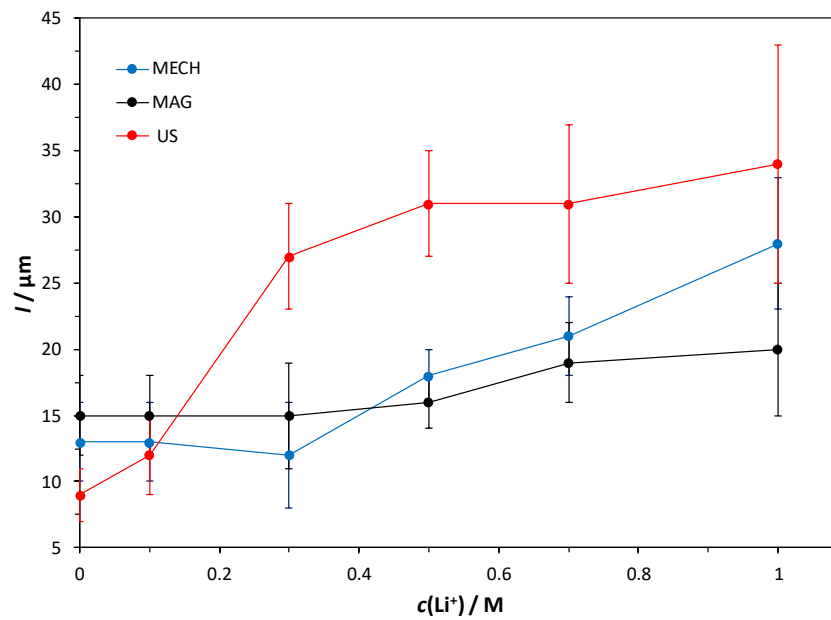
Figure SI10. The average particle sizes of calcite crystals obtained after 5 days of aging in the precipitation systems, $c_i(CaCl_2) = c_i(NaHCO_3) = 0.1$ mol dm^{-3}, plotted as a function of different initial LiCl concentrations. Different initial stirring modes have been applied.

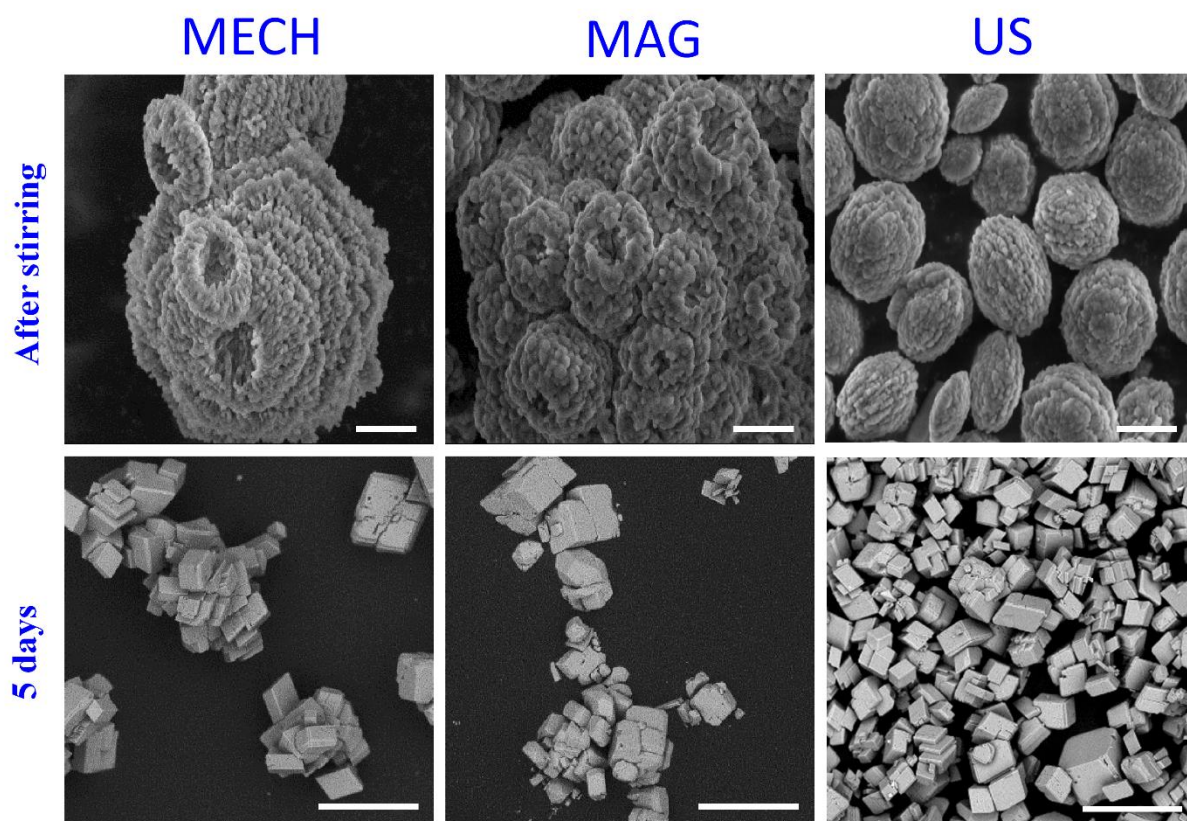**Figure SI11.** Scanning electron micrographs of calcium carbonate samples obtained in the precipitation systems, $c_i(CaCl_2) = c_i(NaHCO_3) = 0.1$ mol dm^{-3}, no lithium addition and after the initial stirring period of one hour for MECH and MAG and 10 minutes for US (top row), scale bar = 2 μm. Precipitate obtained after 5 days of aging (lower row), scale bar = 30 μm.
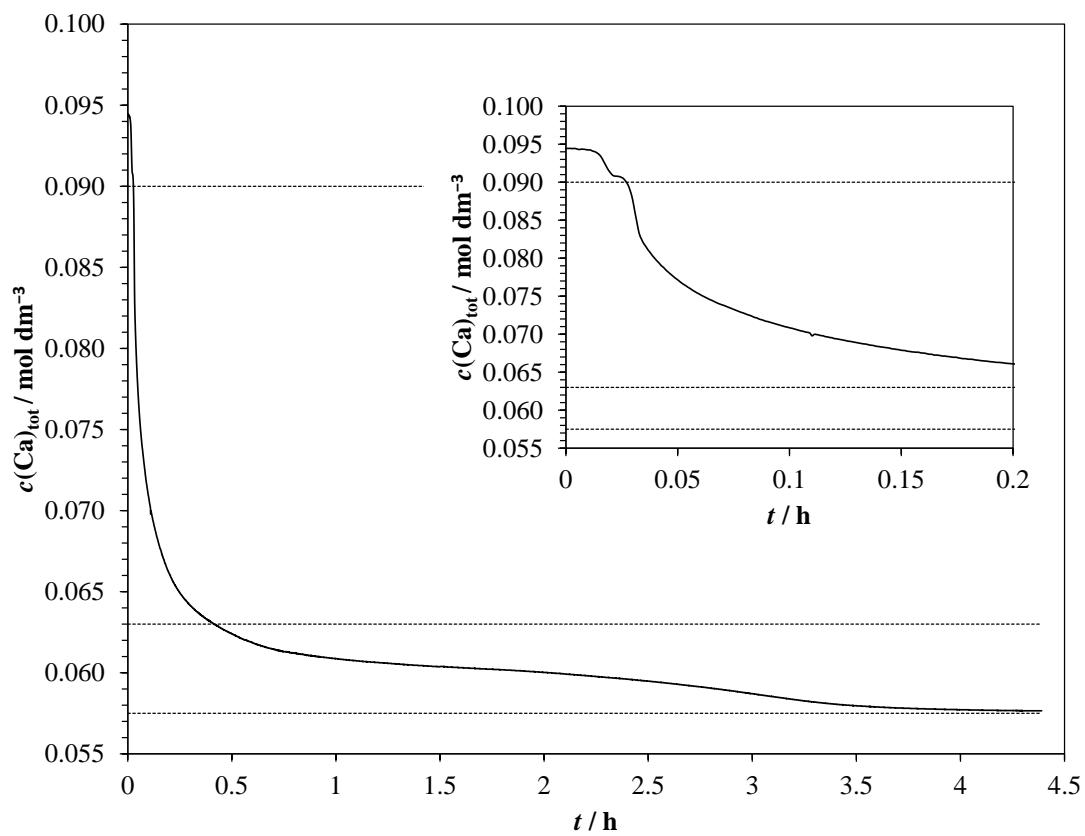
Figure SI12. Progress curve, solution concentration vs. time, of the spontaneous precipitation and transformation of calcium carbonate in the precipitation system $c_i(CaCl_2) = c_i(NaHCO_3) = 0.1$ mol dm^{-3} and no LiCl addition. Insert shows initial 12 minutes of the precipitation process.
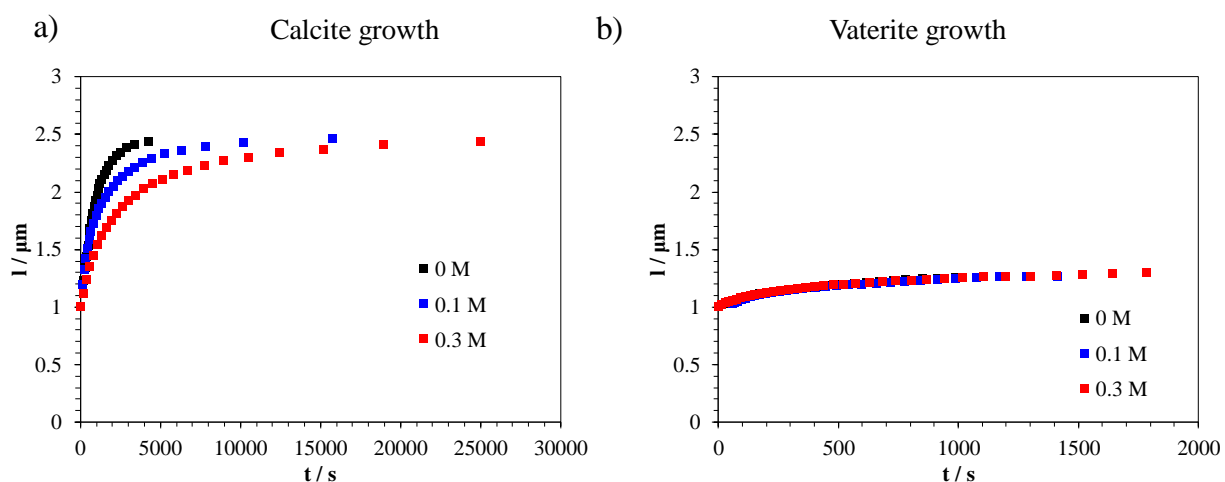
Figure SI13. Change of the initial length ($l_o = 1$ μm) of calcite crystal edge (a) and the radius of the vaterite particle (b) vs. time in the crystal growth experiments. The initial crystal size of the seed used in crystal growth experiments was $l_0 = 1$ μm. The mass concentrations or calcite and vaterite were, γ(calcite) = 125 mg L^{-1} and γ(vaterite) = 125 mg L^{-1} respectively.
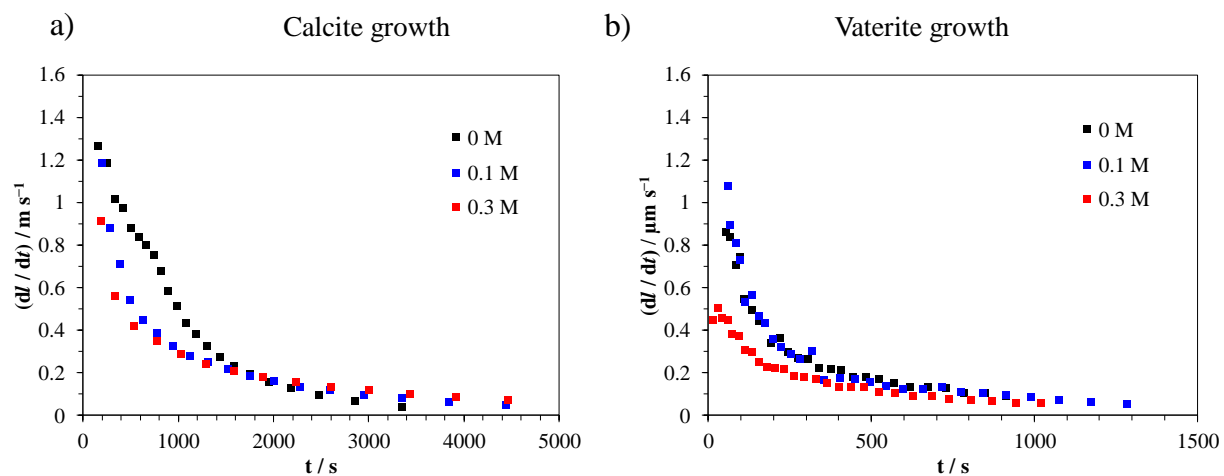
Figure SI14. Plot of growth rates (d*l*/d*t*) as a function of time for the calcite (a) and vaterite (b) crystal growth experiments. The mass concentrations or calcite and vaterite were, γ(calcite) = 125 mg L^{-1} and γ(vaterite) = 125 mg L^{-1} respectively.